GA–A26374

DIAGNOSTIC TESTS, UNUSUAL EXPERIMENTS AND PERFORMANCE ON THE DIII-D GYROTRON SYSTEM

by

J. LOHR, M. CENGHER, I.A. GORELOV, P.B. PARKS, D. PONCE, D. YOUNG, P. JOHNSON, and K. THOMPSON

JANUARY 2009

GENERAL ATOMICS

DISCLAIMER

GA–A26374

DIAGNOSTIC TESTS, UNUSUAL EXPERIMENTS AND PERFORMANCE ON THE DIII-D GYROTRON SYSTEM

by

J. LOHR, M. CENGHER, I.A. GORELOV, P.B. PARKS, D. PONCE, D. YOUNG,*
P. JOHNSON,† and K. THOMPSON‡

This is a preprint of a synopsis of a paper presented at the 7th International Workshop on Strong Microwaves: Sources and Applications, July 27 through August 2, 2008, in Nizhny, Novgorod, Russia, and to be published in the *Proceedings.*

*National Renewable Energy Laboratory, Golden, Colorado.
†Butler University, Indianapolis, Indiana.
‡University of Wisconsin, Madison, Wisconsin.

Work supported in part by
the U.S. Department of Energy
under DE-FC02-04ER54698 and DE-FG02-89ER53296

GENERAL ATOMICS PROJECT 30200
JANUARY 2009

GENERAL ATOMICS

DIAGNOSTIC TESTS, UNUSUAL EXPERIMENTS AND PERFORMANCE ON THE DIII-D GYROTRON SYSTEM

J. Lohr, M. Cengher, I.A. Gorelov, P.B. Parks, D. Ponce, D. Young,[a] P. Johnson,[b] and K. Thompson[c]

General Atomics, PO Box 85608, San Diego, California 92186-5608, USA
[a]National Renewable Energy Laboratory, Golden, Colorado, USA
[b]Butler University, Indianapolis, Indiana, USA
[c]University of Wisconsin, Madison, Wisconsin, USA

The gyrotron complex on the DIII-D tokamak now has been completed with the installation of six 110 GHz gyrotrons in the 1.0 MW class. The rf pulse lengths have been limited administratively to 5.0 s at full parameters, 40 A, 80 kV, and over 10.3 MJ per pulse at peak power, ~3.1 MW, has been injected into DIII-D for plasma experiments on a single shot using 5 gyrotrons. The reliability of the gyrotron performance has been 82% over a three-year period and was 85.5% in 2008.

A direct high power measurement of the transmission line efficiency has been made. The total efficiency averaged 74% for the 31.75 mm diam. evacuated corrugated transmission lines carrying the $HE_{1,1}$ waveguide mode past 7 miter bends. Loss in the Matching Optics Unit (MOU) was 3.3%–7.9% and a fairly large loss, ~10% was measured in the first sections of waveguide after the MOU.

Three materials experiments have been performed using the system. The power from one gyrotron was used to flash anneal amorphous silicon, forming aligned single crystals suitable as nucleation sites for CVD deposition of silicon leading to high efficiency photovoltaic conversion at low cost. A similar annealing of CMOS structures produced improved junctions accessing the 32 nm performance node. Finally, a gyrotron-pumped waveguide loaded with naptha and Ni powder is being used to investigate the possibility of creating high velocity frozen deuterium pellets driven by rapidly expanding gas heated by microwaves.

In this paper we report on the status, history and applications of the 110 GHz six gyrotron system installed on the DIII-D tokamak. The gyrotrons have been used with excellent reliability in a wide range of experiments and the installation has developed into a standard component of the auxiliary heating system on DIII-D, in use on most experimental days. The tubes have injected over 10 MJ on a single plasma shot, with rf pulses up to 5 s in length. The nominal pulse length limit is 10 s, however, as will be discussed later, the calculated collector fatigue lifetime depends not only on the number of pulses but also on their duration, therefore the pulse lengths used in experiments have been limited administratively to 5 s, which is consistent with present experimental requirements. All the tubes except one have been tested to 1.0 MW output. The sixth tube, for reasons believed to be connected with poor electron beam quality from the cathode, was only able to be operated at 750 kW output for 5 s pulses. One of the other tubes is being reconditioned to full power after repair of a vacuum leak.

Three of the gyrotrons, all the tubes in the first production run, experienced collector failures, which now are understood to have been due to excessive power loading in the collector. New operating procedures and hardware are predicted to extend the collector lifetime to about 50,000 pulses 5 s in length, which should be adequate for the long term experimental program on DIII-D.

The gyrotron and power supply installation will be described, including the results of direct measurements of the transmission line efficiencies. Alignment and setup procedures will be presented in connection with the efficiency measurements and system reliability data for the past five years, which demonstrate the high reliability in support of experiments will be shown. The collector failures and remedial steps will be discussed, followed by a description of launcher performance, including damage to one launcher mirror. The change in emphasis of the workshop from focusing on strong microwaves in plasmas to the broader subject featuring both sources and applications will be addressed in descriptions of a number of materials processing experiments, which have been done using the gyrotron installation during times when it was not being used for fusion research. Finally, the long term plans for enhancements to the DIII-D gyrotron installation will be presented.

System Description, Reliability and Transmission Line Efficiency

The gyrotron complex on the DIII-D tokamak has been described previously [1]. There are six gyrotrons, all in the 1 MW class at 110 GHz, which are connected to the tokamak with circular 31.75 mm diameter corrugated evacuated waveguides up to 100 m in length (Fig. 1). The only window in a line is the gyrotron CVD diamond window. At the tokamak there are three launcher assemblies, each of which can independently direct the beams from two gyrotrons to anywhere in the tokamak upper half plane and ±20º toroidally for current drive.

The gyrotrons are all diode tubes [2] and are powered by vacuum tetrode modulator/regulators that provide a reproducible applied voltage of 80 kV ±500 Vdc and modulation frequencies up to 10 kHz. The power supply configuration is shown schematically in (Fig. 2). Because regulation at precise voltages is compromised by changes in such factors as ambient temperature, changes in the unregulated kV supply voltage during plasma shots and pulse length, the gyrotrons must be tuned slightly for a given set of experimental conditions. This is done, for example, by making slight changes in the main magnetic field, by adjusting the filament voltage, by adjusting the magnetic field in the gun region or by boosting the filament voltage at a predetermined time before the gyrotron pulse. Once the tuning is set, the gyrotron operation is rather reliable, achieving an overall average greater than 80% success rate (defined as the number of times individual gyrotrons produced the pulse length requested divided by the total number of requests) over the past five years (Fig. 3). During acceptance testing the gyrotrons are operated at maximum possible output power, at about 31% efficiency, and must achieve 10 consecutive 5.0 s pulses at $P_{gen} \geq$ 1.0 MW without a fault to be accepted. But for plasma experiments, with changing pulse length requests, varying ambient conditions and uncontrollable pulse repetition frequencies based on experimental exigencies, the gyrotrons are operated with slightly detuned parameters. This is usually done by increasing the main magnetic field by as little as 0.2% above the value that delivers peak power and reduces the generated power to about 900 kW.

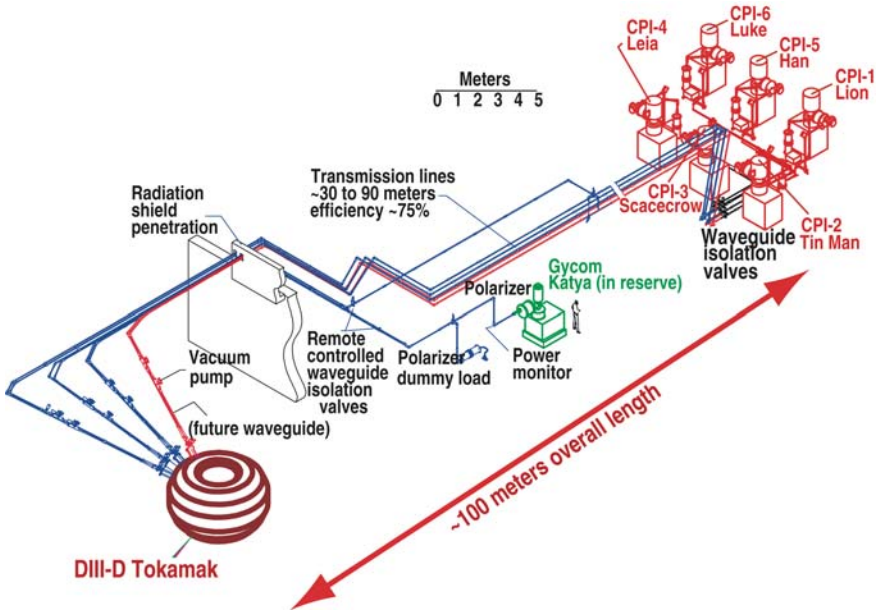

FIG. 1. Isometric layout of the DIII-D gyrotron complex. Six tubes are in operation, injecting >3 MW 110 GHz microwave power into the tokamak over a waveguide line up to 100 m in length with an average of 75% transmission line efficiency. The long term plan calls for a total of eight gyrotrons, each of which will generate 1.5 MW.

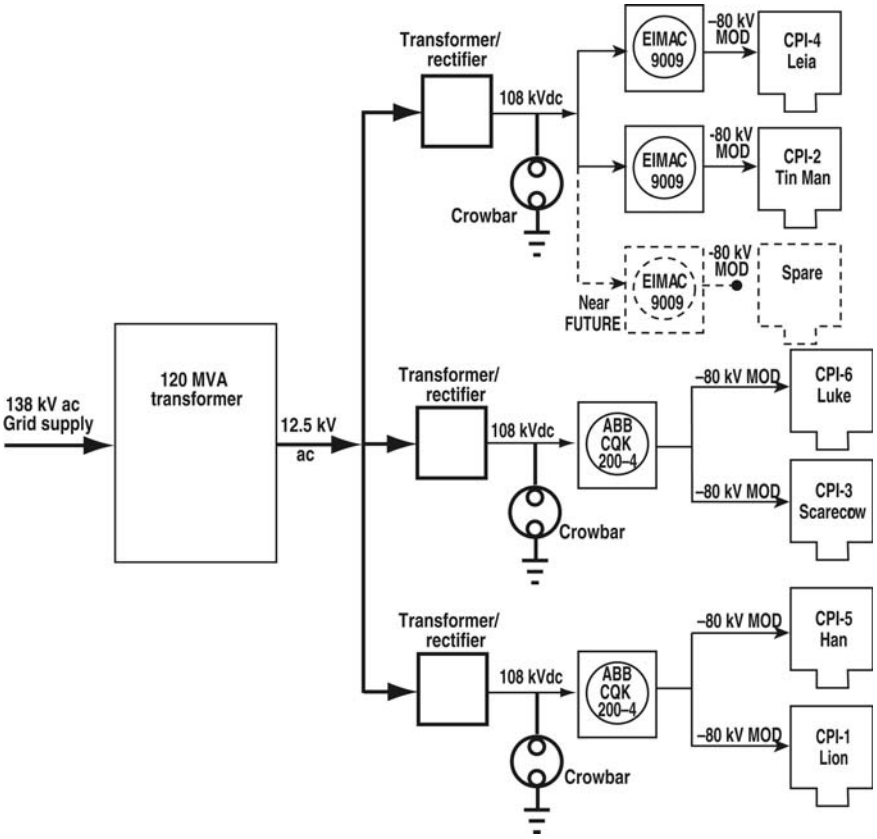

FIG. 2. Schematic diagram of the high voltage power supply system for the DIII-D ECH complex. Vacuum tetrodes are used, driving gyrotrons either singly or in pairs. Ignitron crowbars with microsecond response time and <10 J maximum arc energy protect the gyrotrons.

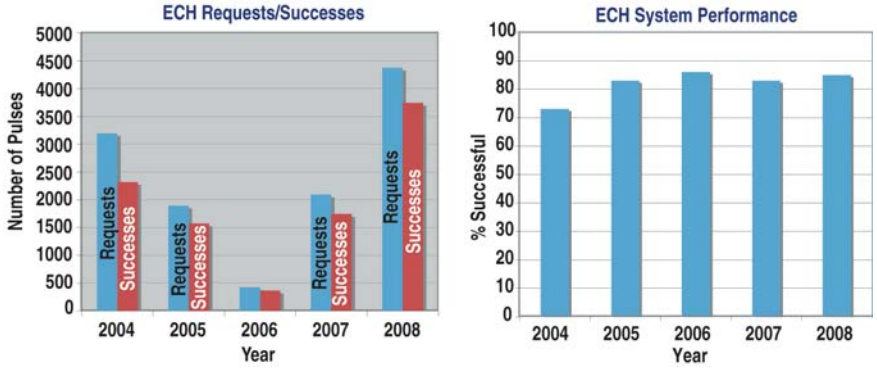

FIG. 3. The ECH system reliability has exceeded 80% for 4 consecutive years despite the constant upgrades and power supply development. In 2008 there were over 4000 requests for individual gyrotron pulses and over 3500 successful pulses which satisfied the requests. A wide variety of pulse lengths, aiming and modulation combinations were used. The system is a regular part of nearly all experiment plans.

The long-term plan calls for an upgrade to 12 MW generated rf power. Two waveguide lines will be added, bringing the total to eight lines. A systematic replacement of the 1 MW class diode gyrotrons to 1.5 MW depressed collector units, all operating at 110 GHz, will then be accomplished.

During the recent experimental period, gyrotrons were added to the system as they became available and extensive modifications to the power supplies were constantly made, which contributed to lowering the reliability. With groups of two gyrotrons being operated from each of two high voltage power supplies, a fault in either gyrotron of a pair will terminate both gyrotron pulses. This reduces the reliability statistics disproportionately. During the 2008 DIII-D campaign, the gyrotron system was being used in support of experiments on most run days, with 4400 requests and over 3700 successes. The most common fault has been when rf generation stops, particularly for long pulses or when tuning up for modulation. A new fault processing system based on field programmable gate array (FPGA) technology is being installed and will permit retries after many of the common faults, which should improve the reliability.

The rf power delivered from each of the gyrotrons to the tokamak has been measured in a number of ways [3] and is the subject of continuing work to reconcile the theoretical waveguide efficiencies with experimental results. Low power tests on complete lines (Fig. 4) showed that, for a pure $HE_{1,1}$ waveguide mode, the line losses were about -1 dB, or 20%, in good agreement with a theoretical estimate [4] of -0.84 dB calculated for a line having 12 miter bends with 1.6% loss per miter. During these measurements, 10-m long sections of the waveguides were subjected to 1 m displacements with no detectable change in transmission efficiency. But for high power, the waveguide losses have been higher than for the cold tests, about -1.25 dB. High power measurements of the transmission line efficiencies made for the long section of the waveguide, up to 90 m, with 10 miter bends gave losses consistent with the cold test measurements on similar sections of the waveguides. The additional losses were accounted for in the first several meters of the lines following the injection point, including about 5 miter bends. These losses, averaging about 80 kW, were measured using resistance temperature devices (RTDs) attached to the waveguides and an infrared camera viewing these parts of the lines covered with black electricial tape used to bring the emissivity up to about 1.0. Because the additional losses occur in the first several meters of waveguide beyond the injection point and are not seen in low power tests when a pure $HE_{1,1}$ mode is excited, mode conversion to lossy modes occurring as a result of imperfect alignment or non-Gaussian content of the injected rf beam is suspected for the losses.

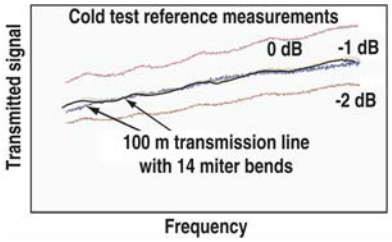

Present Hot Test Measurments

Gyrotron	MOU loss	Calculated line loss	Total line loss
CPI-3 Scarecrow	3.8%	20.2% (-0.98 dB)	28.3% (-1.45 dB)
CPI-1 Lion	3.3%	20.2% (-0.98 dB)	26.0% (-1.30 dB)
CPI-4 Leia	7.9%	20.2% (-0.98 dB)	30.7% (-1.59 dB)
CPI-5 Han	4.5%	20.2% (-0.98 dB)	21.2% (-1.03 dB)

FIG. 4. Low power tests with pure $HE_{1,1}$ modes gave about -1 dB transmission line efficiency in agreement with theory. High power measurements on four of the systems, on the other hand, showed higher losses of about 0.5 dB, which are believed to be due to mode conversion arising from slight misalignment of the rf beam as it enters the waveguide. The frequency was swept for the low power tests to eliminate possible errors due to resonances.

When a gyrotron is first received, short rf pulses are launched into free space and the power profiles are measured at intervals of about 10 cm for the first meter after the beam exits the gyrotron window. These power profiles are then analyzed by a phase retrieval algorithm [5], which yields not only the mode mixture in the beam, but also the x-y offset of the peak of the Gaussian at the gyrotron window and its off-perpendicular propagation direction. Typically these are a few millimeters offset and $\leq 0.5^{o}$ off-perpendicular. In order to place the center of the beam on the axis of the transmission line system, a specially designed spool piece with offset, non-parallel flanges is made, which aligns the beam and the MOU axis. The slight tilt in the whole MOU assembly with respect to horizontal which results from this process

is accommodated by making the first 2 or 3 meters of waveguide slightly flexible by corrugating their outer surfaces. The cold tests previously described had shown that a slight bend over this distance made no detectable change in the propagation loss. But the use of a single coupling mirror makes it impossible to achieve complete flexibility in the injection geometry. By translating the single mirror along the original rf beam direction toward and away from the gyrotron it is possible to adjust the beam position in the horizontal, but not the vertical, plane, while tilting the mirror in the horizontal and vertical planes can change the angle at which the beam approaches the waveguide. When the beam is centered on the waveguide, therefore, it is possible that a small non-coaxiality in the vertical plane is present.

Assessment of the alignment is being made in three ways. The 1st of these will be real time measurements of power absorbed in a dummy load located close to the injection point, about 3 m and two miter bends after injection. The dummy load power should be maximized when the beam is well-aligned with the waveguide axis. The 2nd measurement technique uses the power radiated from a gap in the waveguide located at an odd multiple of one quarter of the beat wavelength between $HE_{1,1}$ and $HE_{2,1}$ propagating modes. The beat wavelength, L, in our 31.75 mm diameter waveguides at 110 GHz is 817 mm, therefore the measurement can be made using a waveguide gap power monitor [1] located, for example, at 5L/4 or 1021.5 mm from the injection point. At this point, a 0.1º off-coaxial injection will result in a 10% differential in the radiated power in the plane defined by the injected rf beam and the waveguide axis. The third measurement is a variation of the second in which the rf beam is relaunched into free space after propagating an odd multiple of one quarter of the beat wavelength described in the second technique. When the rf is relaunched into free space after traversing several meters of guide, the mode content can be determined using infrared power measurements and phase recovery analysis based on the power profiles. Alternatively, the coaxiality of the rf beam can also be inferred from the location of the beam center at any odd multiple of a quarter of the beat wavelength from the injection point in free space, again using an infrared camera to locate the center of the rf beam with respect to the waveguide axis.

Using the more standard technique of simply measuring the power in the waveguide lines at two locations separated by long waveguide runs containing 8–10 miter bends, the transmission line efficiencies in Fig. 4 were determined. The losses in the lines measured in hot tests and cold tests are consistent with each other except that in hot tests there is an additional loss of about -0.5 dB, which is indicated by heating of the first few meters of waveguide and the first 4 or 5 miter bends. As discussed above, we believe that this loss arises from slight misalignment of the Gaussian beam at the input to the waveguide. For 31.75 mm diam waveguide at 110 GHz, a transverse offset of 1.0 mm with perfectly co-axial injection will result in 1% mode conversion from $HE_{1,1}$ and a 0.1º deviation from perfectly co-axial injection with no transverse offset will result in 0.4% mode conversion [6,7]. In the real case, the injected rf beam will have a combination of these injection errors making it difficult to determine the exact mode structure, a combination of $HE_{1,1}$ and other modes, which will be excited in the guide. Although some of these modes, the $HE_{2,1}$ for example, will propagate in corrugated circular guide with nearly the same low loss as $HE_{1,1}$, they will lead to additional mode conversion at the first few miter bends in the lines, with heating of the waveguides in both the forward and reflected directions from the miters.

Collector and Launcher Mirror Failures

Initial operation of the 1 MW gyrotrons was done with allowable collector power loading up to 1 kW/cm^2. This loading turned out to be excessive and resulted in fatigue failures of the collectors on the first three gyrotrons placed in service. The electron beam footprint is smallest and the collector power density is highest when the electron beam is low in the collector during axial sweeping. Following the failures, the fatigue calculations were improved, with the result that a reduced standard for allowable collector loading, 600 W/cm^2, was determined. To achieve this, the electron beam was raised about 10 cm in the collector, increasing the footprint; the sweep frequency was increased from 4 to 5 Hz; and the dwell time at the limits of the sweep was reduced by a combination of an increase in the available output volt-

age of the power supply driving the sweep magnet to 200 V and by employing a sawtooth waveform for the sweeping magnetic field, which opposes the fringing field of the superconducting magnet. The fatigue lifetime is determined both by the number of single pulses and the number of repetitive sweep cycles, both of which contribute to the stress in the collector OFHC copper. Increasing the sweep frequency reduces the stress slightly, while increasing the number of sweep cycles per unit pulse length, resulting in a moderate improvement in lifetime. A direct measurement of the effect of these measures on the sweeping magnetic field inside the gyrotron is shown in Figs. 5 and 6, indicating in particular that the dwell time at the low point in the sweep is reduced by ≈40%. The new operational procedures have increased the predicted collector lifetime to 50,000 pulses 5 s in length.

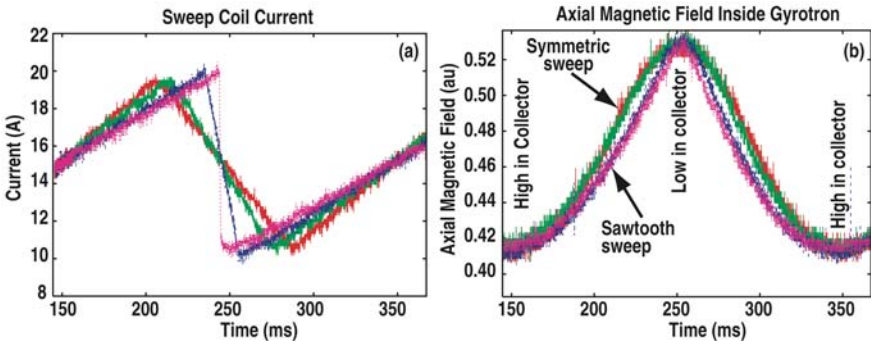

FIG. 5. Changing the sweep coil waveform from symmetric to a sawtooth reduced the dwell time of the electron beam at its lowest point in the collector by about a factor of two.

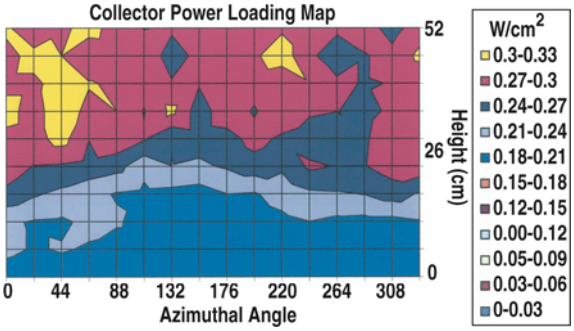

FIG. 6. The electron beam was also raised by about 10 cm in the collector, greatly reducing the power loading where the beam footprint is smallest and the power loading is greatest. The power loading is thus maintained <600 W/cm^2 everywhere in the collector.

The steerable launchers in the DIII-D system have two mirrors on each waveguide line. The rf beam expands from a 62.5 mm diam waveguide and is incident on a weakly focusing mirror at a 45º angle. From this mirror, the beam strikes a flat surface mirror, which can be moved so that the rf beam is directed over a range ±20º horizontally, in the current drive direction, and poloidally over the tokamak upper half plane, which also involves a 40º range of motion. The mirrors are cooled by radiation and conduction without active cooling. The focus mirrors are made from stainless steel with a thin, 0.125 mm, copper overcoating. The steerable mirrors are made from a multi-layer laminate of stainless steel and copper with a thin copper-reflecting surface. The designs employ stainless steel to add strength and reduce forces during disruptions and copper to reduce resistive heating by the rf beam.

On both of these mirror designs, there is evidence of excessive heating and one of the focus mirrors failed with complete melting of the copper coating and of the stainless steel substrate over a surface area

several mm in diameter. The rf power loading on the copper surface is about 100 W/cm^2 but on stainless steel it is about 5300 W/cm^2, so once the copper layer had melted and exposed the stainless steel, further damage was inevitable. Initial damage was noted during a short vent of the tokamak, but when the tokamak was opened for maintenance following a period during which 269 additional rf pulses had been fired on the damaged line, the damage was found to have spread to >1 cm diam and the stainless steel substrate was melted to a depth of 2 mm (Fig. 7). Heating of the steering mirror by plasma radiation is a significant effect [8], but the reflecting surfaces of the focus mirrors are facing away from the plasma and are not heated significantly by radiation. Although a test program leading to 10 s pulse lengths had been planned, the mirror damage necessitated a redesign effort and a delay in pulse extension beyond 5 s.

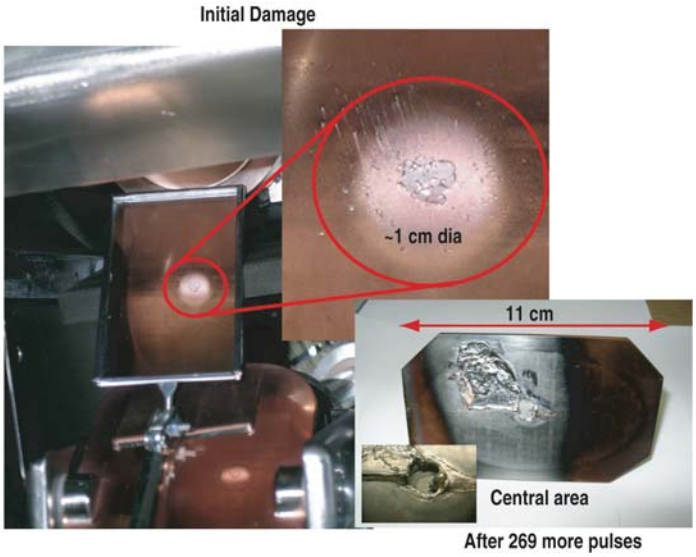

FIG. 7. Photographs of the melt damage to one of the focus mirrors. Once the copper overcoating was breeched, further damage was inevitable. The initial melting was observed in situ using a mirror.

Model calculations revealed that the melt damage could be explained if the braze of the stainless steel mounting stud (Fig. 8) on the back of the focus mirror had formed an incomplete bond to the stainless steel mirror body, thus reducing the conduction away from the center of the mirror. The new design for this mirror will use a Cr-Zr-Cu stud with additional care in making the braze. These measures are predicted to reduce the peak temperature of the mirror surface for 10 s pulses by about 200ºC, to a peak temperature for a 10 s pulse of 820ºC, providing a 200ºC margin against melting the copper.

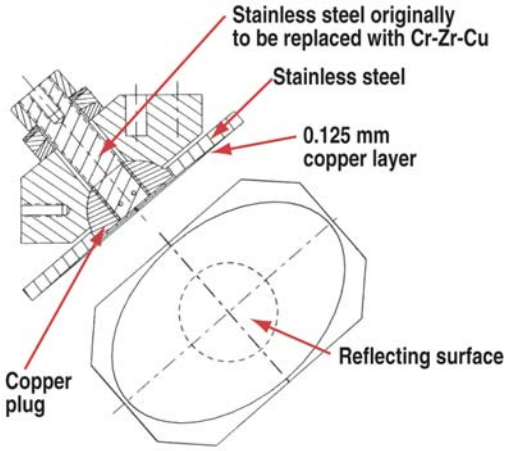

FIG. 8. The focus mirror stainless steel mounting stud will be replaced by Cr-Zr-Cu in the new design.

Microwave Annealing and Heating

Amorphous silicon. The DIII-D gyrotron complex has been used for a number of experiments unrelated to fusion, but which are connected to applications of strong microwaves. The most successful of these have involved rapid heating and crystallization of amorphous silicon leading to improved photovoltaic conversion efficiency and rapid annealing of CMOS structures formed by implantation.

For photovoltaic conversion, high efficiency at low cost is a key factor. Typical solar cells use amorphous silicon on a variety of substrates and have a conversion efficiency of ~8%. With this efficiency, photo-voltaics cannot compete economically with other sources of electricity except in specific applications where the standalone capability of the cells to provide electricity, such as in remote locations or where power requirements are low, take particular advantage of the unique characteristics of the cells. If crystalline or polycrystalline silicon can be produced economically, the competitiveness of photovoltaics will improve, since crystalline silicon has approximately twice the conversion efficiency of the amorphous state. We have subjected amorphous silicon layers on glass to rapid heating [9] using 110 GHz high power microwaves from the DIII-D ECH system and formed excellent silicon crystals in squat, egg shaped pillars about 20 μm in diameter distributed over the surface of the glass (Fig. 9). With these pillars serving as nucleation sites for additional CVD deposited silicon, it is possible that a low cost high efficiency solar cell can be fabricated.

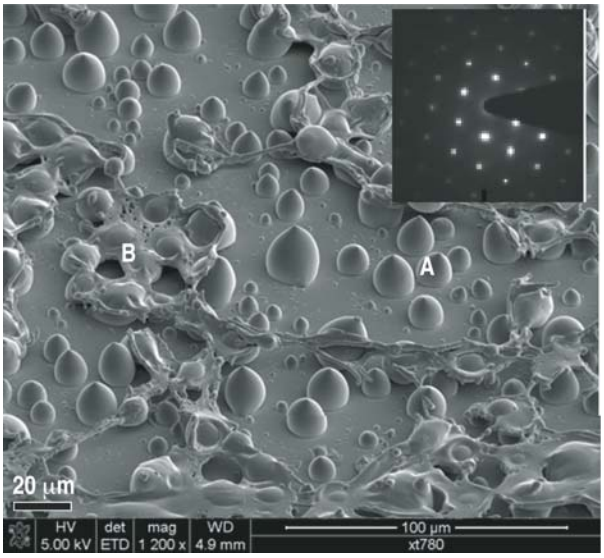

FIG. 9. Sample seen with field emission scanning electron microscopy following microwave annealing. The pillars have very high silicon crystalline quality as verified by the transmission electron microscopy picture shown in the inset. The pillars are about 20 μm in diameter. Target preparation on the glass substrate is indicated in the left side of the figure.

The glass substrates were prepared by coating with a ~120 nm layer of SiO_2 followed by a 1–2 μm thick layer of a-Si:H deposited by hot wire CVD from silane gas at a high rate of 10–100 Å/s. Square samples 2.5 cm on a side were placed in a vacuum chamber where microwave power launched from an open ended waveguide and reflected from a specially designed mirror to provide a flattened power profile irradiated the samples. The power density at the samples was ~40 kW/cm^2 and resulted in rapid heating, at 10^5–10^6 ºC/s, of the silicon to melting temperature of ~1450ºC using pulses ≤8.5 ms in length. The samples were examined using a number of crystallographic techniques including field emission scanning electron microscopy, selected area diffraction and energy dispersive x-ray spectrocscopy. The pillars have excellent crystallinity with only occasional structural defects and very large grain size, ~20 μm. This compares with a grain size of ~1 μm for traditional solid phase crystallization or low frequency microwave annealing

In the next series of experiments, attempts will be made to improve the wetting of the substrate surface by the molten silicon. The characteristics of silicon layers deposited onto the annealed substrates also will be investigated to determine if the annealed crystalline structures can force crystalline alignment of what would normally be an amorphous layer applied by CVD after formation of the pillars.

CMOS structures. A similar series of annealing experiments was performed on CMOS structures originally formed by low energy implantation [10]. During implantation, the specific range of dopants striking crystalline silicon can produce high performance junctions with very small-scale size capable of meeting the requirements of the 32 nm technology node planned for availability through 2013 by the International Technology Roadmap for Semiconductors (ITRS) [11]. But the implantation damages the silicon lattice structure, resulting in an increase in resistivity and decrease in device performance. The conventional solution to this problem is to anneal the structure using flash lamps, however if this is done over a time long compared with diffusion times of the dopants, the scale length of the junctions forming the source/drain and channel regions will increase during the annealing, dopant density will decrease, the performance will be impaired and the requirements of the roadmap cannot be met. One measure of device performance is the contact resistance, which must remain low, and the electrical isolation at small junc-

tion depth, which must remain high. Flash annealing of the structures by microwave heating provides a solution meeting the requirements.

The experiment was very similar to the silicon annealing work described above except that the targets were crystalline silicon with a variety of dopants and geometries. On DIII-D, one of the 110 GHz gyrotrons was easily able to provide heating rates to $5x10^{5o}$C/s up to and beyond the melting point of silicon. The optimum method found empirically was application of a 4.5 ms pulse providing 4 kW/cm^2, which heated the sample to ~1300ºC at about $2.75x10^{5o}$C/s. Subsequent analysis showed that little dopant diffusion occurred during this time period even if the sample was exposed to multiple pulses with a cooldown time between pulses. Electrical activation of the implanted dopants showed a sheet resistance, R_S, of 495–750 Ohms/square for junction depth between 14–2 nm and successive pulses resulted in continual improvements in R_S. The result was ultra shallow junctions which were superior to competing anneal technologies and which satisfied the ITRS requirements at least through 2013. Competing with the implantation/anneal technology is small-scale x-ray photolithography using wavelengths of 0.1–0.8 nm, which has the capability, particularly for the shorter wavelengths, of producing 3D structures. Both techniques can produce excellent performance.

Gyrotron pellet accelerator. A waveguide containing a substance that can be vaporized by microwaves could be used to generate high pressures and temperatures capable of driving pellets suitable for fueling in a fusion device [12]. A preliminary experiment was done using the DIII-D gyrotron complex. A waveguide with diameter 4 mm and length 25 mm was connected to a standard 31.75 mm diam corrugated waveguide using a downtaper. A diamond window in the larger waveguide isolates the test setup from the gyrotron. The small waveguide, isolated from the larger guide by a sapphire window, was filled with napthalene containing an admixture of 1%–5% Ni particles with scale size ~2 μm. This sealed waveguide was surrounded by a thick walled chamber hydro tested to 90 atm and capable of withstanding 680 atm. The microwaves, 500 kW, ~1–2 ms, were directed into the waveguide and were absorbed by the metal particles, which in turn heated the napthalene, which then vaporized producing high temperatures, >1000ºC, and pressures up to approximately 60 atm. In this experiment transducers measured the temperatures and pressures and following the termination of the rf pulse, the napthalene simply recondensed.

In the first attempt at the experiment, electric field enhancement at the interface between the napthalene and sapphire window isolating the small diameter waveguide resulted in arcing at the window surface, with damage to the window and protective termination of the rf pulse due to reflected rf power [13]. It is likely that the match can be improved by use of proper geometry at the window. This area will be redesigned and then the experiment will be tried again.

Conclusion

The ECH complex at DIII-D now has six operating gyrotrons, which have been used both for fusion and for materials experiments. Reliability has been very good and is expected to improve once all power supplies and other enhancements have been installed. The longer term plan is to add two more gyrotrons and waveguide lines with their ancillary equipment and then upgrade to 12 MW generated power by replacing the present group of 1.0 MW diode gyrotrons with depressed collector tubes having unit output power of 1.5 MW.

Acknowledgment

This work was supported by the U.S. Department of Energy under DE-FC02-04ER54698.

References

1. *Lohr, J., et al.,* Fusion Sci. Technol. **48**, 1226 (2005).
2. *Felch, Kevin, et al.,* IEEE Trans. Plasma Sci. **24**, 558 (1996).

3. *Cengher, M., et al.*, Proc. of 15th Joint Workshop on Electron Cyclotron Emission and Electron Cyclotron Heating, J. Lohr, ed., World Scientific, Singapore (2009).
4. *Doane, J.L. and Moeller, C.P.*, Int. J. Electronics **77**, 489 (1994).
5. *Denison, D.R., et al.,* IEEE Trans. on Plasma Sci. **27**, 512 (1999).
6. *Doane, J.L.*, Infrared and Millimeter Waves **13**, 123 (1985).
7. *Ohkubo, K., et al.,* Proc. of 10th Joint Workshop on Electron Cyclotron Emission and Electron Cyclotron Heating, T. Donné and T. Verhoeven, eds, World Scientific, Singapore, 597 (1997).
8. *Lohr, J., et al.,* Proc. Int. Workshop Strong Microwaves in Plasmas 2005, A.G. Litvak, ed., **2,** 434, Russian Academy of Sciences, Nizhny Novgorod (2006).
9. *Liu, F., et al.,* "Ultra-high Crystalline-quality Silicon Pillars Formed by Millimeter-wave Annealing of Amorphous Silicon on Glass," submitted to Nature Materials (2008).
10. *Thompson, K., et al.,* J. Vac. Sci. Technol. B **23**, 970–978 (2005).
11. International Roadmap for Semiconductors (ITRS), Presentations from the 2007 ITRS Winter Conference, Makuhari Messe, Japan, are available at http://www.itrs.net/Links/2007Winter/2007_Winter_Presentations/Presentations.html.
12. *Parks, P.B. and Perkins F.W.*, Proc. of 33rd EPS Conf. on Plasma Phys., ECA **30I** (2006) P-1.121.
13. *Callis, R.W., et al.,* Fusion Energy 2008 (Proc. 22nd Int. Conf., Geneva, 2008) (Vienna: IAEA) Paper FT/P2-23, http://www-pub.iaea.org/MTCD/Meetings/fec2008pp.asp